Ion Pairing and Redissociaton in Low Permittivity Electrolytes for Multivalent Battery Applications

Journal:	*The Journal of Physical Chemistry Letters*
Manuscript ID	jz-2020-003344.R1
Manuscript Type:	Letter
Date Submitted by the Author:	18-Feb-2020
Complete List of Authors:	Self, Julian; University of California Berkeley Department of Materials Science and Engineering, Materials Science and Engineering Hahn, Nathan; Sandia National Laboratories, Nanoscale Sciences Fong, Kara; University of California, Berkeley, Chemical Engineering McClary, Scott; Purdue University, Davidson School of Chemical Engineering Zavadil, Kevin; Sandia National Laboratories, 1874 Persson, Kristin; E O Lawrence Berkeley National Laboratory, Energy Technologies Area; UC Berkeley, Materials Science and Engineering

Ion Pairing and Redissociaton in Low Permittivity Electrolytes for Multivalent Battery Applications

Julian Self,[†,‡] Nathan T. Hahn,[¶] Kara D. Fong,[§,‡] Scott A. McClary,[¶] Kevin R. Zavadil,[¶] and Kristin A. Persson[*,†,‡]

†*Department of Materials Science and Engineering, University of California, Berkeley*
‡*Energy Technologies Area, Lawrence Berkeley National Laboratory*
¶*Material, Physical, and Chemical Sciences Center, Sandia National Laboratories*
§*Department of Chemical and Biomolecular Engineering, University of California, Berkeley*

E-mail: kapersson@lbl.gov

Abstract

Detailed speciation of electrolytes, as a function of chemical system and concentration, provides the foundation for understanding bulk transport as well as possible decomposition mechanisms. In particular multivalent electrolytes have shown a strong coupling between anodic stability and solvation structure. Furthermore, solvents that are found to exhibit reasonable stability against alkaline earth metals generally exhibit low-permittivity which typically increases the complexity of the electrolyte species. To improve our understanding of ionic population and associated transport and in these important classes of electrolytes, the speciation of $MgTFSI_2$ in monoglyme and diglyme systems are here studied via a multiscale thermodynamic model using first principles calculations for ion association and molecular dynamics simulations for dielectric properties. The results are then compared to Raman and dielectric relaxation (DRS) spectroscopies, which independently confirm the modeling insights. We find that the significant presence of free ions in the low permittivity glymes in concentration ranges from 0.02 M to 0.6 M is well explained by the low permittivity redissociation hypothesis. Here, salt speciation is largely dictated by long-range electrostatics, which include permittivity increases due to polar contact-ion pairs. The present results suggest that other low permittivity multivalent electrolytes may also reach high conductivities due to redissociation.

Main Text

One of the impediments towards improving Mg electrochemistry is the lack of the fundamental understanding of the governing electrochemical and physiochemical properties of the electrolyte. Although there exists a significant body of work focusing on transport properties, solvation and electrochemical stability,[1–6] ion pairing and speciation remain poorly understood for commonly studied multivalent electrolyte systems,[7] despite their crucial importance to overall electrolyte behavior. A critical leap in understanding is needed in multivalent electrolytes to accelerate their development and achieve parity with lithium electrolytes.

Most Li-ion and specifically high-permittivity electrolytes studied for electrochemical applications exhibit a decreasing *molar* conductivity as a function of concentration,[8] as ion-pairing and viscosity increase. In contrast, multivalent electrolytes (which are generally prepared with solvents of low static permittivity,[2] e.g. $\epsilon < 10$) can show an increasing molar conductivity Λ (concentration normalized conductivity) versus concentration. More precisely, in

concentration ranges of electrochemical interest (e.g. 0.01 M to 1 M), the molar conductivity initially increases and eventually reaches a maximum at moderate concentrations. The initial increase in molar conductivity for multivalent low permittivity electrolytes may be due to a dramatic, more complex change in ion speciation as compared to monovalent high-permittivity electrolytes.

Two representative low permittivity multivalent Mg^{2+} electrolytes are $MgTFSI_2$ (Mg bis(trifluoromethylsulfonyl)imide) in monoglyme (G1) and $MgTFSI_2$ in diglyme (G2), which are widely investigated electrolytes for use in electrochemical cells,[2] primarily due to their high conductivity, solubility and commercial availability. This anion-solvent combination is also widely utilized for Li-Oxygen and Li-Sulfur electrochemistry.[9–11] However, $MgTFSI_2$ in ethers requires additional salt (e.g. $MgCl_2$) in order to allow plating and stripping at high Coulombic efficiencies.[2] Nonetheless, the present work will focus specifically on $MgTFSI_2$ in ethers without additional salt, as even such simple electrolytes, which are the subject of intense research and interest,[3,4,6,12,13] are still poorly understood in terms of salt speciation[14] and bulk thermodynamic properties.[15]

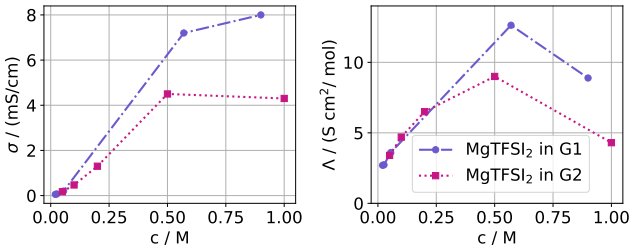

Figure 1: Measured conductivity (left) and molar conductivity (right) as a function of $MgTFSI_2$ salt concentration in G1 or G2 solvents.

For both $MgTFSI_2$ in G1 and G2, concentration dependent molar conductivity deviates from that of high permittivity electrolytes (Figure 1).[15,16] The molar conductivity increases with concentration, indicating non-conventional behavior: typically (e.g. for high permittivity solvents) molar conductivity decreases as a function of concentration in the dilute limit following Kohlrausch's law,[17] and at concentrations ~ 0.5 M following, among other factors, significant viscosity and ion pairing increases.[18] The molar conductivity increase for G1 and G2 suggests that ion pairing decreases[13] (i.e. the population fraction of charge carriers is increased), contrary to what would be expected from simple predictions based on the law of mass action.

Salama et al. suggested from diffusion and Raman measurements that $MgTFSI_2$ in G1 exists primarily as free ions, independent of concentration,[15] a finding under contention.[6,7] Similarly, Kubisiak and Eilmes[12] reported MD simulations which showed strictly solvent-solvated Mg^{2+} from 0.1 M to 1 M $MgTFSI_2$ in G1. Sa et al. studied $MgTFSI_2$ in G2, and found (an unusual) increase in diffusivity of salt from 0.1 M to 0.7 M by an order of magnitude, which is suggested as resulting from a "complicated solution environment at different ionic strengths".[16] Using MD they found a significant presence of SSIPs or free ions, and monotonically increasing ion-pairing with concentration from 0.2 M to 2 M. Unfortunately, the results from Salama et al., Kubisiak and Eilmes and Sa et al. are not consistent with the relevant molar conductivity increase. Lapidus et al.,[6] via X-ray and MD studies of 0.4 M $MgTFSI_2$ in G2, found approximately half of Mg^{2+} was free, with the remaining split into contact ion pairs (CIPs) or neutral triple ions. Kimura et al., who studied $MgTFSI_2$ in triglyme via conductivity and Raman, suggested a shifting equilibrium between solvent-separated ion pairs (SSIPs) and free ions as concentration is varied to explain the increasing molar conductivity, without providing a physical motivation for such a mechanism.[13] The differences in the aforementionned interpretations and suggestions illustrate that no clear consensus has yet emerged regarding the speciation in low permittivity multivalent systems.

We hypothesize that the interplay between ion pairing and molar conductivity can be rationalized via redissociation.[19–23] In low permittivity electrolytes, associated salt species tend to form due to the strong electrostatic interac-

tions compared to polar solvents.[24] If these associated species are endowed with a significant dipole moment, they will increase the total permittivity via an increase in the orientational polarizability and favor a larger population of dissociated salt species as concentration increases, a phenomenon termed *redissociation*.[21,22,25] Previous work on studying the interplay between permittivity increase and ion association has focused on monovalent salts.[19,21–23,25–27] To the best of the authors' knowledge, redissociation has not been analyzed or proposed for non-aqueous multivalent systems, despite the inherently stronger electrostatic interactions present.

Characterization of ion pairing for multivalent liquid electrolytes systems is quite challenging due to the strong interionic interactions in solution: many conventional techniques such as conductometry are often not directly applicable,[24] and the challenges are compounded for low permittivity systems. In order to evaluate the redissociation hypothesis for low permittivity multivalent electrolytes, we herein use a multiscale computational model (MSM) to predict permittivity and salt speciation as a function of concentration. To verify the results, we undertake Raman and dielectric relaxation spectroscopy (DRS). While previous work on combined permittivity and speciation diagrams have used a posteriori experimental data,[23,28,29] the current MSM is entirely theoretically and computationally based, and relies on experimental input only for validation. Furthermore, a significant number of dielectric relaxation studies have been carried out on monovalent low permittivity systems,[19,21,26,27] as well as some high-permittivity multivalent systems,[28] however none yet on multivalent low permittivity electrolytes — the subject of the present work.

For a system with divalent cations and monovalent anions, the concentration association constant K_A directly provides the concentration ratio of associated monocationic contact ion pairs $c_{cip,+}$ to free ions c_{++} and c_- via the following relationships:[24]

$$K_A(c) = \frac{c_{cip,+}}{c_{++}c_-} = K_A^0 \frac{y_{++}y_-}{y_{cip}} f_{\epsilon,A} \qquad (1)$$

In the above equation, the thermodynamic association constant K_A^0 is introduced, as well as the concentration activity coefficients of the multivalent cation, anion, and contact ion pair y_{++}, y_{--} and $y_{cip,+}$ and the permittivity correction term $f_{\epsilon,A}$. K_A^0 accounts for specific short range interactions while the activity coefficients y_i as well as the permittivity correction term $f_{\epsilon,A}$, account for long-range non-specific electrostatic interactions.

Assuming only free ions and contact ion pairs then the following concentration conservation equation can be written:

$$c = c_{++} + c_{cip,+} \qquad (2)$$

Moreover, charge neutrality imposes the following condition:

$$2c_{++} + c_{cip,+} = c_- \qquad (3)$$

In the present work, K_A^0 is obtained through first-principles electronic structure calculations within a continuum solvation model enhanced with an explicit first solvation shell for the multivalent cation (see Methods). For low to moderate concentrations (e.g. up to 0.7 M), a Guggenheim - type equation is often used for activity coefficients,[28] where the first term is the Debye-Huckel expression, employed in the present work, as follows:[28,30]

$$\frac{y_{++}y_-}{y_{cip,+}} = 10^{\frac{-4A_{DH}\sqrt{I}}{1+B_{DH}\alpha_{DH}\sqrt{I}}} \qquad (4)$$

In the above equation, the symbols have their typical significance,[28,30] where B_{DH} is the Debye-Huckel term, α_{DH} is the distance of closest approach, A_{DH} is the Debye-Huckel parameter and I is the ionic strength. While Guggenheim - type expressions also include linear and higher order terms in ionic strength for the ions' chemical potential, here we assume that additional terms to the standard Debye-Huckel expression impact first order due to changes in permittivity.[31,32] Thus, the role of such terms is fulfilled by $f_{\epsilon,A}$, described above. Hence, we neglect any higher order corrections.

If the permittivity of the electrolyte remains fairly constant as a function of concentration,

then $f_{\epsilon,A}$ would equal unity. However, if the permittivity changes appreciably, as it tends to for low permittivity electrolytes, then the following phenomenological equation can be used,[19] where b is a positive phenomenological constant:[19]

$$f_{\epsilon,A} = exp(\frac{-b}{\epsilon(c=0)} + \frac{b}{\epsilon(c)}) \quad (5)$$

With increasing concentration of charged species, the y_i charged species activity coefficients decrease, hence competing with the mass action law which promotes association. If the permittivity increases, then this will act as an additional driving force for reduced association (and increased association if the permittivity decreases). Together, equations 1, 2, 3, 4 and 5 allow for construction of speciation diagrams from first principles calculations provided $\epsilon(c)$ is known in the desired concentration range.

$$\epsilon(c) = \epsilon(c=0) + \sum_i \Delta\epsilon_i c_i + O(c_i c_j) \quad (6)$$

In equation 6, the concentration - dependent permittivity is equal to the permittivity of the neat solvent $\epsilon(c=0)$ in addition to the dielectric increment per species $\Delta\epsilon_i$ multiplied by the concentration of said species c_i. $\Delta\epsilon_i$ is here independent of concentration, and it is also assumed that higher order terms can be neglected. If coupled to equations 1-5, then the total permittivity can be calculated as a function of concentration, provided each $\Delta\epsilon_i$ is known. As described in the methods, and in a previous publication,[33] $\Delta\epsilon_i$ can be calculated from classical molecular dynamics simulations.

Figure 2 (top) shows the static permittivity (dielectric constant) as a function of concentration and the speciation as a function of concentration (bottom) for $MgTFSI_2$ in G2. The static permittivity is computed to increase from 7.4 (neat G2) to 14.8 (0.5 M), while it is measured to increase from 7.4 to 16.2. There is good agreement throughout the studied concentration range (0.02 M to 0.5 M). The error bars are a consequence of the fitting procedure required to extract the static permittivity values from

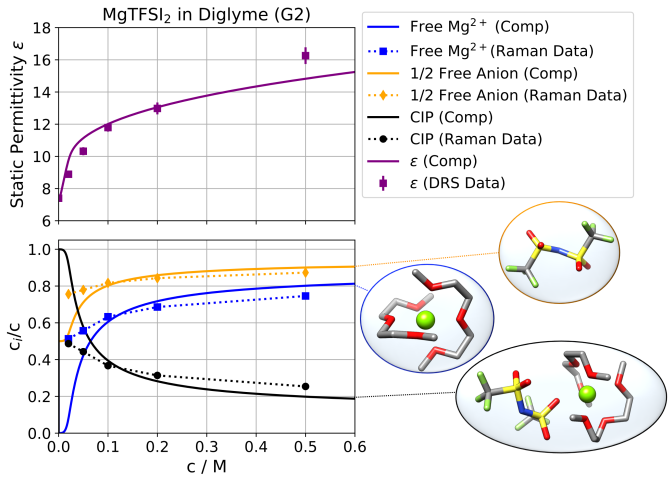

Figure 2: Permittivity (top) and speciation diagram (bottom) of $MgTFSI_2$ in G2 at 25°C. Computed species fraction c_i/c is shown with solid lines, except for the anion which is shown for 0.5 c_i/c. Species in question are illustrated in bubbles.

the frequency dependent spectra (see Methods). The tendency of the permittivity to increase with concentration is different than salts in typical high permittivity electrolytes (e.g. NaCl in water) where the dielectric constant typically decreases with concentration due to the loss of free solvent molecules bound into the solvation shell of free ions, thus reducing the orientational polarizability of the solution.[34] Here, the increase in permittivity with concentration unequivocally indicates that associated species, e.g. CIPs, which hold a strong dipole moment, are present in appreciable quantities in the solution.

The speciation inferred from the Raman analysis of TFSI ion pairing is in good agreement with the computed values (Figure 2, bottom). Here, the population fraction of free ions increases with concentration, while the associated species, e.g. CIPs, decrease, consistent with the molar conductivity increase.

Table 1 shows the computed dielectric increment per salt species, which was used in the MSM. We note that the presence of free ions tends to lower ϵ, however, the decrease is much less than the increase in ϵ from associated species (CIP).

Figure 3 shows the static permittivity as a

Table 1: Computed dielectric increment per mole of species, and computed K_A^0

solvent	$\frac{\Delta\epsilon_{++}}{1M}$	$\frac{\Delta\epsilon_{--}}{1M}$	$\frac{\Delta\epsilon_{CIP,+}}{1M}$	K_A^0
G2	-11	-3.0	147	5.2×10^8
G1	-13	-2.7	72	3.6×10^8

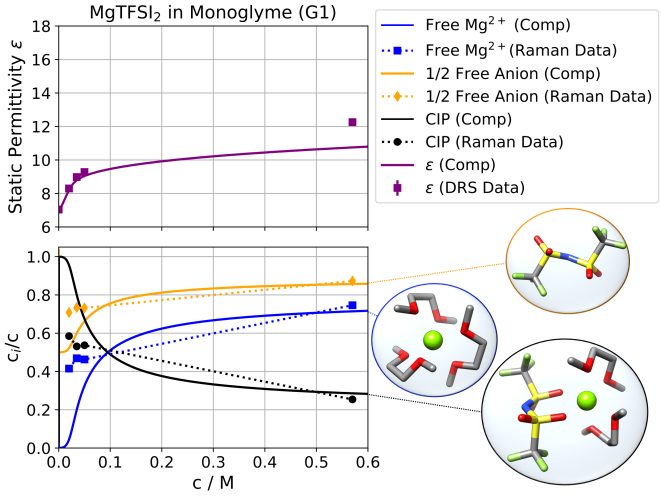

Figure 3: Permittivity (top) and speciation diagram (bottom) of $MgTFSI_2$ in G1 at 25°C. Computed species fraction c_i/c is shown with solid lines, except for the anion which is shown for 0.5 c_i/c. Species in question are illustrated in bubbles.

function of concentration (top) and the speciation as a function of concentration (bottom) for $MgTFSI_2$ in G1. The static permittivity is computed to increase with concentration, from 7.0 (neat G1) to 10.8 (0.57 M salt in G1), and is measured to increase from 7.0 to 12.3 by DRS, in general agreement. No data points were obtained between 0.05 M and 0.57 M due to the miscibility gap in the electrolyte[15] (see Methods).

The bottom panel of Figure 3 shows the speciation as a function of concentration. The Raman analysis of associated $TFSI^-$ populations is consistent with the trends: the fraction of associated salt (CIPs) generally decreases with concentration and fraction of free ions increases with concentration, qualitatively similar to the $MgTFSI_2$ in G2 system. The high concentration population experimental data (0.57 M) are within 5 % of the computed values, but the lower concentrations do not show such agreement. The disagreement suggests that either the computed K_A is overestimated in the lower concentrations, or there could be presence of higher order aggregates (e.g. solvent separated ion pairs, triple ions), which is discussed futher below. The Raman data points indicate a slight increase in ion-pairing from 0.035 M to 0.05 M by 0.6 %. However, the error estimate for Raman inferred populations due to instrument noise is 6 % in the lowest concentration (0.02 M), and otherwise generally decrease with increasing concentration (error bars are not displayed here for visual clarity, see SI). Thus, the emphasis is here placed on the general trend of decreasing ion-pairing with concentration.

At high concentrations, the permittivity of G2 electrolytes is higher than that of G1, despite a similar fraction of ion pairing according to Raman spectroscopy, and this highlights an important difference in CIP structure tendencies. As shown in Table 1, CIPs in G2 show a much larger dielectric increment increase than G1 (147/M versus 72/M), which allows the electrolyte to reach a higher static permittivity despite having a similar fraction of CIPs. The larger dielectric increment is due to a preference for the more polar monodentate configuration of the CIP in G2, in contrast to the bidendate majority configuration of the CIP in G1 (see inset illustrations in Figure 3). In the model used herein, we approximate the majority dentation as the only ion-pair structure, although likely some admixture of both dentations is present in both liquids.The K_A^0s for both studied systems (G2 and G1) are on the order of 10^8 (Table 1), while for high permittivity electrolytes typically K_A^0s are much smaller (e.g. on the order of 10^2).[28] The concentration - dependent K_As are dramatically lowered from the permittivity increase, a phenomenon specific to low permittivity systems.

As part of the presented results, a few possible sources of errors should be considered and discussed. First, the assumption of a concentration - independent interionic distance parameter α_{DH} could in principle be improved.[35] In this work we derive α_{DH} as the sum of radii[36,37] of a CIP and an anion, providing a reasonable

value for a multivalent Mg^{2+} system.[35] Second, assuming CIPs as the only associated species is certainly an approximation, especially in the low concentration regime. For previous multivalent systems, SSIPs were shown to be present at low concentrations (below 0.2 M),[28] which may explain the disagreement at low concentration for the $MgTFSI_2$ in G1 and G2 systems. Unfortunately, the low frequency limit of DRS, and the Raman analysis methods (which cannot distinguish between free ions and SSIPs, and show higher errors at lower concentrations), preclude us from directly investigating the presence of SSIPs in this work. Moreover, the agreement between the MSM with DRS and Raman analysis at higher concentrations supports the assumption of CIPs as the majority associated species at higher concentrations.

Importantly, for both G1 and G2 electrolyte systems, the calculated values for permittivity and speciation and the respective experimental data are consistent with the redissociation hypothesis. More precisely, the permittivity increase, in addition to the increasing ionic strength, which enhances screening of free ions and lowers their chemical potential (via equation 4), explain the dramatic stabilization of free ions at higher concentrations.

In contrast to high-permittivity Li-ion electrolytes, multivalent electrolytes for battery applications, which generally use low permittivity solvents show an increasing molar conductivity versus concentration. To improve our understanding of the complex speciation in these liquids, we use modeling and DRS, to establish an increase in static permittivity as a function of salt concentration in $Mg(TFSI)_2$/G1 and G2 electrolytes. Furthermore, the speciation diagrams constructed from the multiscale modeling methodology show an increase in the fraction of dissociated species with concentration, which is confirmed experimentally by Raman spectroscopy. The combined evidence strongly indicates that polar contact ion-pairs that form at low concentration trigger a redissociation mechanism, leading to an increase in free, charge-carrier ions at higher concentrations. For G1, the dramatic change in speciation from redissociation may also play a role in the miscibility gap from 0.05 M to 0.57 M.[15] Furthermore, the current results suggest that for multivalent low permittivity electrolytes, redissociation is a non-specific effect (i.e. independent of the salt chemistry), provided a considerable population of strongly polar associated species persists. Preliminary measurements indicate that many Mg^{2+} and Ca^{2+} electrolytes of interest exhibit increasing molar conductivity with concentration, and further investigations linking these observations to the attendant cluster structures and populations will be the subject of future publications. Finally, the ability to tune redissociation - and therefore speciation and transport - via designer salt additives remains a viable path forward.

Methods

Infinite dilution association constants K_A^0, shown in Table 1, were calculated via first principles quantum chemistry calculation. Hybrid-DFT calculations were undertaken with Gaussian 016 software[38] using ωb97x-d[39] with the def2tzvp basis,[40] with a continuum solvation model[41] (CSM) using the neat solvent permittivity, as well as an first explicit solvation shell for cations. Before geometry optimization via ab initio methods, initial configurations were picked via conformational analysis using MacroModel[42] and an OPLS-based force field,[43] where structures with dentation matching those from the classical molecular dynamics were picked. In order to correct for spurious contributions of low frequency modes to the vibrational partition function, Truhlar's[44] correction was applied using Patton's code.[45] $f_{\epsilon,A}$ was calculated using the optimized geometries of the neat solvent and then single point calculations as the permittivity of the CSM is varied. A function as described by equation 5 was fit (further details in SI). This yielded an analytic function allowing the computation of the correction to the association constant due to the change in permittivity.

In order to calculate $\Delta\epsilon_i$ molecular dynamics calculations were undertaken with GROMACS,[46] with details following those of a previ-

ous manuscript.[33] Briefly, each simulation held a single salt species in a box of solvent, such that the concentration was 0.1 M. In order to include the contribution of salt species to the total permittivity, via the fluctuation dissipation theorem, the dipole of the salt species had to be drawn and included in the total polarization. This was undertaken with in house code, described and provided in a previous publication.[33] As was necessary, certain of the simulations carried an overall charge, which, for which the GROMACS software provided a correcting background homogeneous charge.[46,47] For charged associated salt species, the net charge was subtracted at the center of mass.[46] Briefly, the dipole moment P of the associated salt species can be written as follows:

$$P_{salt\ species,x} = \Sigma_{ions} q_{ions} r_x \quad (7)$$

In the above equation, *ions* refers to the atomic point charges of the salt species and x the given cartesian direction. If the associated salt species has an overall charge, then the center of mass (COM) charge can be subtracted:

$$P'_{salt\ species,j} = P_{salt\ species,j} - r_{COM}(\Sigma_k q_k) \quad (8)$$

Electrolyte solutions for ionic conductivity, DRS, and Raman measurements were prepared in an argon-filled glove box with $H_2O < 1$ ppm and $O_2 < 0.1$ ppm (MBraun). The solvents G1 (1,2-dimethoxyethane) and G2 (diethylene glycol dimethyl ether) were purchased in anhydrous form from Millipore-Sigma, distilled, and stored over 3 Å molecular sieves with activated alumina. $MgTFSI_2$ (Solvionic, 99.5%) was dried under vacuum at 170°C for a minimum of 48 h prior to use. It was found that the dissolved $MgTFSI_2$ salt imparted a non-trivial solution volume increase over that of the pure solvents and thus careful measurement of overall solution volume was required to achieve accurate molarity values. This is particularly important for solutions of moderate to high concentration. Consistent with a previous report, we find that $MgTFSI_2$/G1 solutions exhibit a significant miscibility gap between ∼0.05 M and ∼0.57 M, precluding measurements at intermediate concentrations.[15]

Solution ionic conductivities were measured in the aforementioned glove box using AC impedance incorporating a home-made conductivity probe consisting of two parallel Pt electrodes. The cell constant of this conductivity probe was periodically calibrated in KCl solutions of various concentrations to ensure measurement accuracy.

Raman spectroscopy was performed in sealed vials on a WITec Confocal Raman Microscope using a 532 nm excitation laser. The TFSI speciation was measured through careful spectral fitting of the TFSI breathing mode region (∼740 cm^{-1}) using Gaussian/Lorentzian line shapes, similar to published methods.[5,48] Select examples are shown in the supporting information document (SI).

Dielectric spectra were measured in glass vials using an immersed slim-form coaxial probe (Keysight N1501A) and vector network analyzer (Keysight P9375A) over a frequency range from 0.5 to 26.5 GHz. Multiple measurements were made to ensure repeatability, and various immersion depths were tested to confirm the absence of associated artifacts. Calibration was maintained and periodically refreshed through an ECal module (Keysight N7555A). A three-point calibration was performed before each DRS series using air, short-circuit, and tetrahydrofuran.[49] During spectral acquisition, the samples were briefly exposed to air (< 1 min). However, no subsequent changes were observed in DRS measurements repeated after long-term exposure to air, indicating that the measurement is insensitive to electrolyte air exposure over these time-scales. DRS data were fit with two Debye relaxations for G1 electrolytes, and one Cole-Cole and one Debye relaxation for G2 electrolytes[50–52] (Further details in Supporting Information).

Acknowledgments

This work was supported by the Joint Center for Energy Storage Research, an Energy Innovation Hub funded by the U.S. Department of Energy. Work at Lawrence Berkeley Na-

tional Laboratory was supported by the Assistant Secretary for Energy Efficiency and Renewable Energy, under Contract No. DEAC02-05CH11231. We thank the National Energy Research Scientific Computing Center (NERSC) for computing resources, as well as NIH grant S10OD023532. Sandia National Laboratories, is a multimission laboratory managed and operated by National Technology and Engineering Solutions of Sandia, LLC., a wholly owned subsidiary of Honeywell International, Inc., for the U.S. Department of Energy's National Nuclear Security Administration under contract DE-NA-0003525.

Supporting Information

Further details on DRS and Raman analysis, as well as the MSM, provided in the Supporting Information.

References

(1) Shterenberg, I.; Salama, M.; Gofer, Y.; Levi, E.; Aurbach, D. The Challenge of Developing Rechargeable Magnesium Batteries. *MRS Bulletin* **2014**, *39*, 453–460.

(2) Attias, R.; Salama, M.; Hirsch, B.; Goffer, Y.; Aurbach, D. Anode-Electrolyte Interfaces in Secondary Magnesium Batteries. *Joule* **2019**, *3*, 27–52.

(3) Shterenberg, I.; Salama, M.; Yoo, H. D.; Gofer, Y.; Park, J.-B.; Sun, Y.-K.; Aurbach, D. Evaluation of $(CF_3SO_2)_2N$ (TFSI) Based Electrolyte Solutions for Mg Batteries. *Journal of The Electrochemical Society* **2015**, *162*, A7118–A7128.

(4) Ha, S.-Y.; Lee, Y.-W.; Woo, S. W.; Koo, B.; Kim, J.-S.; Cho, J.; Lee, K. T.; Choi, N.-S. Magnesium(II) Bis(trifluoromethane sulfonyl) Imide-Based Electrolytes with Wide Electrochemical Windows for Rechargeable Magnesium Batteries. *ACS Applied Materials & Interfaces* **2014**, *6*, 4063–4073.

(5) Giffin, G. A.; Moretti, A.; Jeong, S.; Passerini, S. Complex Nature of Ionic Coordination in Magnesium Ionic Liquid-Based Electrolytes: Solvates with Mobile Mg^{2+} Cations. *The Journal of Physical Chemistry C* **2014**, *118*, 9966–9973.

(6) Lapidus, S. H.; Rajput, N. N.; Qu, X.; Chapman, K. W.; Persson, K. A.; Chupas, P. J. Solvation Structure and Energetics of Electrolytes for Multivalent Energy Storage. *Phys. Chem. Chem. Phys.* **2014**, *16*, 21941–21945.

(7) Rajput, N. N.; Seguin, T. J.; Wood, B. M.; Qu, X.; Persson, K. A. *Modeling Electrochemical Energy Storage at the Atomic Scale*, springer ed.; 2018; pp 79–124.

(8) Yamada, Y.; Yamada, A. Review-Superconcentrated Electrolytes for Lithium Batteries. *Journal of The Electrochemical Society* **2015**, *162*, A2406–A2423.

(9) Aurbach, D.; Pollak, E.; Elazari, R.; Salitra, G.; Kelley, C. S.; Affinito, J. On the Surface Chemical Aspects of Very High Energy Density, Rechargeable Li–Sulfur Batteries. *Journal of The Electrochemical Society* **2009**, *156*, A694.

(10) Burke, C. M.; Pande, V.; Khetan, A.; Viswanathan, V.; McCloskey, B. D. Enhancing electrochemical intermediate solvation through electrolyte anion selection to increase nonaqueous Li–O_2 battery capacity. *Proceedings of the National Academy of Sciences* **2015**, *112*, 9293–9298.

(11) Rosenman, A.; Markevich, E.; Salitra, G.; Aurbach, D.; Garsuch, A.; Chesneau, F. F. Review on Li-Sulfur Battery Systems: an Integral Perspective. *Advanced Energy Materials* **2015**, *5*, 1500212.

(12) Kubisiak, P.; Eilmes, A. Solvation of Mg^{2+} Ions in $Mg(TFSI)_2$-Dimethoxyethane

Electrolytes-A View from Molecular Dynamics Simulations. *The Journal of Physical Chemistry C* **2018**, *122*, 12615–12622.

(13) Kimura, T.; Fujii, K.; Sato, Y.; Morita, M.; Yoshimoto, N. Solvation of Magnesium Ion in Triglyme-Based Electrolyte Solutions. *The Journal of Physical Chemistry C* **2015**, *119*, 18911–18917.

(14) Baskin, A.; Prendergast, D. Exploration of the Detailed Conditions for Reductive Stability of Mg(TFSI) $_2$ in Diglyme: Implications for Multivalent Electrolytes. *The Journal of Physical Chemistry C* **2016**, *120*, 3583–3594.

(15) Salama, M.; Shterenberg, I.; Gizbar, H.; Eliaz, N. N.; Kosa, M.; Keinan-Adamsky, K.; Afri, M.; Shimon, L. J. W.; Gottlieb, H. E.; Major, D. T.; Gofer, Y.; Aurbach, D. Unique Behavior of Dimethoxyethane (DME)/Mg(N(SO_2 CF_3)$_2$)$_2$ Solutions. *The Journal of Physical Chemistry C* **2016**, *120*, 19586–19594.

(16) Sa, N.; Rajput, N. N.; Wang, H.; Key, B.; Ferrandon, M.; Srinivasan, V.; Persson, K. A.; Burrell, A. K.; Vaughey, J. T. Concentration Dependent Electrochemical Properties and Structural Analysis of a Simple Magnesium Electrolyte: Magnesium Bis(trifluoromethane sulfonyl)imide in Diglyme. *RSC Advances* **2016**, *6*, 113663–113670.

(17) Wright, M. R. *An Introduction to Aqueous Electrolyte Solutions*; Wiley, 2007.

(18) J. M. Barthel,; Krienke, H.; Kunz, W. *Physical Chemistry of Electrolyte Solutions: Modern Aspects*, springer science & business media ed.; 1998; Vol. 5.

(19) Delsignore, M.; Farber, H.; Petrucci, S. Ionic conductivity and Microwave Dielectric Relaxation of Lithium Hexafluoroarsenate (LiAsF6) and Lithium Perchlorate (LiClO4) in Dimethyl Carbonate. *The Journal of Physical Chemistry* **1985**, *89*, 4968–4973.

(20) Doucey, L.; Revault, M.; Lautié, A.; Chaussé, A.; Messina, R. A study of the Li/Li+ couple in DMC and PC solvents: Part 1: Characterization of LiAsF6/DMC and LiAsF6/PC solutions. *Electrochimica acta* **1999**, *44*, 2371–2377.

(21) Borodin, O.; Douglas, R.; Smith, G.; Eyring, E. M.; Petrucci, S. Microwave Dielectric Relaxation, Electrical Conductance, and Ultrasonic Relaxation of $LiPF_6$ in Poly(ethylene oxide) Dimethyl Ether-500. *The Journal of Physical Chemistry B* **2002**, *106*, 2140–2145.

(22) Petrucci, S.; Masiker, M. C.; Eyring, E. M. The Possible Presence of Triple Ions in Electrolyte Solutions of Low Dielectric Permittivity. *Journal of Solution Chemistry* **2008**, *37*, 1031–1035.

(23) Logan, E. R.; Tonita, E. M.; Gering, K. L.; Ma, L.; Bauer, M. K. G.; Li, J.; Beaulieu, L. Y.; Dahn, J. R. A Study of the Transport Properties of Ethylene Carbonate-Free Li Electrolytes. *Journal of The Electrochemical Society* **2018**, *165*, A705–A716.

(24) Marcus, Y.; Hefter, G. Ion Pairing. *Chemical Reviews* **2006**, *106*, 4585–4621.

(25) Cavell, E. A. S.; Knight, P. C. Effect of Concentration Changes on Permittivity of Electrolyte Solutions. *Zeitschrift fur Physikalische Chemie Neue Folge* **1968**, *57*, 331–334.

(26) Farber, H.; Petrucci, S. Ultrahigh Frequency and Microwave Relaxation of Lithium Perchlorate in Tetrahydrofuran. *The Journal of Physical Chemistry* **1975**, *79*, 1221–1227.

(27) Farber, H.; Petrucci, S. Electrical Conductance, Ultrasonic Relaxation, and Microwave Dielectric Relaxation of Sodium Perchlorate in Tetrahydrofuran. *The Journal of Physical Chemistry* **1976**, *80*, 327–335.

(28) Eberspächer, P.; Wismeth, E.; Buchner, R.; Barthel, J. Ion Association of Alkaline and Alkaline-earth Metal Perchlorates in Acetonitrile. *Journal of Molecular Liquids* **2006**, *129*, 3–12.

(29) Hwang, S.; Kim, D.-H.; Shin, J. H.; Jang, J. E.; Ahn, K. H.; Lee, C.; Lee, H. Ionic Conduction and Solution Structure in $LiPF_6$ and $LiBF_4$ Propylene Carbonate Electrolytes. *The Journal of Physical Chemistry C* **2018**, *122*, 19438–19446.

(30) Newman, J.; Thomas-Alyea, K. E. *Electrochemical Systems*; John Wiley & Sons, 2012.

(31) Shilov, I. Y.; Lyashchenko, A. K. The Role of Concentration Dependent Static Permittivity of Electrolyte Solutions in the Debye–Hückel Theory. *The Journal of Physical Chemistry B* **2015**, *119*, 10087–10095.

(32) Schlumpberger, S.; Bazant, M. Z. Simple Theory of Ionic Activity in Concentrated Electrolytes. *arXiv:1709.03106 [cond-mat, physics:physics]* **2017**, arXiv: 1709.03106.

(33) Self, J.; Wood, B. M.; Rajput, N. N.; Persson, K. A. The Interplay between Salt Association and the Dielectric Properties of Low Permittivity Electrolytes: The Case of $LiPF_6$ and $LiAsF_6$ in Dimethyl Carbonate. *The Journal of Physical Chemistry C* **2018**, *122*, 1990–1994.

(34) Buchner, R.; Hefter, G. T.; May, P. M. Dielectric Relaxation of Aqueous NaCl Solutions. *The Journal of Physical Chemistry A* **1999**, *103*, 1–9.

(35) Lee, W. H.; Wheaton, R. J. Analysis of Conductance Data for Associated Unsymmetrical Electrolytes. *The Journal of Physical Chemistry* **1978**, *82*, 605–608.

(36) Marcus, Y. Ionic Radii in Aqueous Solutions. *Chemical Reviews* **1988**, *88*, 1475–1498.

(37) Salomon, M. Conductance of Solutions of Lithium Bis(trifluoromethanesulfone)imide in Water, Propylene Carbonate, Acetonitrile and Methyl Formate at 25C. *Journal of Solution Chemistry* **1993**, *22*.

(38) Frisch, M. J. et al. *Gaussian16 Revision B.01*; 2016.

(39) Chai, J.-D.; Head-Gordon, M. Long-range Corrected Hybrid Density Functionals with Damped Atom-Atom Dispersion Corrections. *Physical Chemistry Chemical Physics* **2008**, *10*, 6615.

(40) Weigend, F.; Ahlrichs, R. Balanced Basis Sets of Split Valence, Triple Zeta Valence and Quadruple Zeta Valence Quality for H to Rn: Design and Assessment of Accuracy. *Physical Chemistry Chemical Physics* **2005**, *7*, 3297.

(41) Tomasi, J.; Mennucci, B.; Cammi, R. Quantum Mechanical Continuum Solvation Models. *Chemical Reviews* **2005**, *105*, 2999–3094.

(42) Schrodinger, L. MacroModel. 2018.

(43) Jorgensen, W. L.; Maxwell, D. S.; Tirado-Rives, J. Development and Testing of the OPLS All-Atom Force Field on Conformational Energetics and Properties of Organic Liquids. *Journal of the American Chemical Society* **1996**, *118*, 11225–11236.

(44) Ribeiro, R. F.; Marenich, A. V.; Cramer, C. J.; Truhlar, D. G. Use of Solution-Phase Vibrational Frequencies in Continuum Models for the Free Energy of Solvation. *The Journal of Physical Chemistry B* **2011**, *115*, 14556–14562.

(45) Rodriguez-Guerra, J.; Chen, J. GoodVibes v2.0.2. **2018**, 10.5281/zenodo.1247565, 10.5281/zenodo.1247565.

(46) Abraham, M. J.; Murtola, T.; Schulz, R.; Páll, S.; Smith, J. C.; Hess, B.; Lindahl, E. GROMACS: High Performance Molecular

Simulations Through Multi-Level Parallelism from Laptops to Supercomputers. *SoftwareX* **2015**, *1-2*, 19–25.

(47) Hub, J. S.; de Groot, B. L.; Grubmüller, H.; Groenhof, G. Quantifying Artifacts in Ewald Simulations of Inhomogeneous Systems with a Net Charge. *Journal of Chemical Theory and Computation* **2014**, *10*, 381–390.

(48) Watkins, T.; Buttry, D. A. Determination of Mg^{2+} Speciation in a $TFSI^-$-Based Ionic Liquid With and Without Chelating Ethers Using Raman Spectroscopy. *The Journal of Physical Chemistry B* **2015**, *119*, 7003–7014.

(49) Badiali, J.-P.; Cachet, H.; Cyrot, A.; Lestrade, J.-C. Dielectric Properties of Electrolyte Solutions. Lithium Perchlorate Solutions in Tetrahydrofuran + Benzene Mixtures. *Journal of the Chemical Society, Faraday Transactions 2* **1973**, *69*, 1339.

(50) Cole, K. S.; Cole, R. H. Dispersion and Absorption in Dielectrics I. Alternating Current Characteristics. *The Journal of Chemical Physics* **1941**, *9*, 341–351.

(51) Kremer, F., Schönhals, A., Eds. *Broadband Dielectric Spectroscopy*; Springer Berlin Heidelberg: Berlin, Heidelberg, 2003.

(52) Grosse, C. A Program for the Fitting of Debye, Cole-Cole, Cole-Davidson, and Havriliak-Negami Dispersions to Dielectric Data. *Journal of Colloid and Interface Science* **2014**, *419*, 102–106.

Table of Contents Graphic